



Article scientifique

Article

2012

Accepted version

Open Access

This is an author manuscript post-peer-reviewing (accepted version) of the original publication. The layout of the published version may differ .

---

## The behavioral significance of coherent resting-state oscillations after stroke

---

Dubovik, Sviatlana; Pignat, Jean-Michel; Ptak, Radek; Aboulafia Brakha, Tatiana; Allet, Lara; Gillibert, Nicole; Magnin, Cécile; Albert, Fabien; Momjian-Mayor, Isabelle; Nahum, Louis; Lascano, Agustina Maria; Michel, Christoph; Schnider, Armin; Guggisberg, Adrian

### How to cite

DUBOVIK, Sviatlana et al. The behavioral significance of coherent resting-state oscillations after stroke. In: NeuroImage, 2012, vol. 61, n° 1, p. 249–257. doi: 10.1016/j.neuroimage.2012.03.024

This publication URL: <https://archive-ouverte.unige.ch/unige:19369>

Publication DOI: [10.1016/j.neuroimage.2012.03.024](https://doi.org/10.1016/j.neuroimage.2012.03.024)

## **The behavioral significance of coherent resting-state oscillations after stroke**

*Sviatlana Dubovik<sup>a</sup>, Jean-Michel Pignat<sup>b</sup>, Radek Ptak<sup>a</sup>, Tatiana Aboulafia<sup>b</sup>, Lara Allet<sup>c</sup>, Nicole Gillibert<sup>a</sup>, Cécile Magnin<sup>a</sup>, Fabien Albert<sup>b</sup>, Isabelle Momjian-Mayor<sup>b</sup>, Louis Nahum<sup>a</sup>, Agustina M. Lascano<sup>b</sup>, Christoph M. Michel<sup>b</sup>, Armin Schnider<sup>a</sup>, Adrian G. Guggisberg<sup>a</sup>*

<sup>a</sup> Division of Neurorehabilitation

<sup>b</sup> Division of Neurology, and

<sup>c</sup> Unit of Physiotherapy Research and Quality Assurance, University Hospital of Geneva

\* Correspondence: Dr. Adrian Guggisberg, Division of Neurorehabilitation, Department of Clinical Neurosciences, University Hospital of Geneva, Av. de Beau-Séjour 26, 1211 Geneva 14, Switzerland, Email: aguggis@gmail.com, Phone: +41 22 382 3521, Fax +41 22 382 3644

## **Abstract**

Stroke lesions induce not only loss of local neural function, but disruptions in spatially distributed areas. However, it is unknown whether they affect the synchrony of electrical oscillations in neural networks and if changes in network coherence are associated with neurological deficits. This study assessed these questions in a population of patients with subacute, unilateral, ischemic stroke.

Spontaneous cortical oscillations were reconstructed from high-resolution electroencephalograms (EEG) with adaptive spatial filters. Maps of functional connectivity (FC) between brain areas were created and correlated with patient performance in motor and cognitive scores.

In comparison to age-matched healthy controls, stroke patients showed a selective disruption of FC in the alpha frequency range. The spatial distribution of alpha band FC reflected the pattern of motor and cognitive deficits of the individual patient: network nodes that participate normally in the affected functions showed local decreases in FC with the rest of the brain. Interregional FC in the alpha band, but not in delta, theta, or beta frequencies, was highly correlated with motor and cognitive performance. In contrast, FC between contralesional areas and the rest of the brain was negatively associated with patient performance.

Alpha oscillation synchrony at rest is a unique and specific marker of network function and linearly associated with behavioral performance. Maps of alpha synchrony computed from a single resting-state EEG recording provide a robust and convenient window into the functionality and organization of cortical networks with numerous potential applications.

**Keywords:** neural networks, stroke, neurological deficits, alpha oscillations, functional connectivity

## 1. Introduction

Therapy of brain disease could potentially be improved if we had better knowledge about how brain organization is disturbed after brain damage and how lost functions can be restored. Functional imaging studies can provide important insights into brain physiology and pathology (Cramer, 2008), but the activation and lesion mapping techniques used traditionally have inherent limitations for the study of changes in brain function induced by lesions. Brain lesions induce not only loss of local neural function, but also changes in remote networks (Alstott et al., 2009; Honey and Sporns, 2008) which likely remain undetected when analyzing task-induced activations or lesions of circumscribed brain areas. Moreover, many patients with brain lesions are unable to perform the tasks required for inducing activation of the brain area of interest, because they are impaired exactly in those functions that have to be studied (Weiller et al., 1993).

These limitations can be overcome by imaging techniques which assess the functional connectivity (FC) between different brain regions rather than measuring task-induced activations. Studies using fMRI in healthy humans have shown that spontaneous fluctuations of activity in the resting brain are highly organized and coherent within specific neuro-anatomical systems (Damoiseaux et al., 2006; Fox et al., 2005; Greicius et al., 2003). These patterns of coherence are task-independent and can also be studied at rest (Greicius et al., 2003). The topography of coherence between brain regions observed at rest matches the topography of brain activations induced by corresponding tasks (Vincent et al., 2007; Zhao et al., 2011) and the strength of coupling in a given network is linearly related to behavioral performance in tasks relying on this network (Koyama et al., 2011; Wang et al., 2010). Thus, a careful analysis of coherence (or FC) among neural assemblies gives access to functional brain organization. This approach has the crucial advantage that it takes into account the network character of brain activity. Furthermore, it does not depend on patient cooperation or specific activation paradigms, and is therefore suitable for studies on brain dysfunction and recovery of patients with neurological deficits who are often unable to perform tasks. Indeed, recent studies have confirmed that fMRI measurements of interhemispheric FC reflect motor and cognitive performance in patients with stroke (Carter et al., 2010; He et al., 2007).

The concept of FC can be applied not only to fMRI, but also to magnetencephalography (MEG) (Schoffelen and Gross, 2009) or EEG (Guggisberg et al., 2011). It is particularly fruitful when FC is not calculated between sensor or electrode pairs, but between reconstructions of cortical oscillations obtained with inverse solutions. This approach allows for instance to localize the cortical generators of cortico-muscular interaction (Gross et al., 2001; Guggisberg et al., 2011; Schoffelen et al., 2008), as well as to reconstruct cortical network interactions. Initial direct comparisons between resting-state

networks obtained with fMRI and networks reconstructed from MEG suggested a more lateralized configuration of MEG networks (de Pasquale et al., 2010), but this difference disappeared in studies controlling for distortions of MEG/EEG FC due to spatial leakage of the inverse solutions (Brookes et al., 2011a; Brookes et al., 2011b). Simultaneous recordings of resting-state fMRI and EEG have shown that if the time course of spontaneous EEG oscillations or microstate changes is convolved with a hemodynamic response function and used as regressor for fMRI analysis, the resulting BOLD responses localize to similar distributed networks as found in fMRI network studies (Britz et al., 2010; Jann et al., 2009; Musso et al., 2010). Interestingly, the closest spatial match to fMRI networks was found with EEG/MEG networks reconstructed from slow cortical potentials and beta-/gamma power fluctuations (Brookes et al., 2011b; He et al., 2008). Several recent studies have described possible mechanisms for the striking topographical similarity between rapid EEG/MEG interactions and much slower cortical potentials or fMRI fluctuations. One candidate mechanism (Raichle, 2011) might be the scale-free (fractal) dynamics of neural activity (He et al., 2010; Van de Ville et al., 2010) with cross-frequency phase coupling from very slow cortical potentials [which possibly underlie BOLD fluctuations (He and Raichle, 2009)] to fast high-gamma rhythms (Monto et al., 2008; Osipova et al., 2008; Palva et al., 2005a).

Unlike fMRI, EEG and MEG can capture a rich spectrum of neural oscillations and might therefore reveal additional information on the intrinsic brain organization. However, in contrast to the rather well studied functional meaning of fMRI resting state networks, the behavioral and clinical significance of FC in the different EEG/MEG frequencies is largely unknown. Previous MEG studies in patients with brain tumors showed that local decreases in alpha band (~7.5 to 12.5 Hz) FC between a given tumor part and the rest of the brain were associated with dysfunction of this part, whereas normal or increased alpha band FC were found in functional tumor tissue (Guggisberg et al., 2008; Martino et al., 2011). These observations suggested that the magnitude of interregional MEG/EEG FC might be related to function and hence to behavioral performance or deficits of the patients. Moreover, the behavioral relevance of FC seemed to be dependent on the oscillation frequency. This study therefore aimed to assess the clinical and behavioral significance of the spectrum of EEG FC. Based on previous studies, we hypothesized that stroke lesions disrupt synchronous electrical oscillations at rest and that this disruption is linearly correlated with neurological deficits of the patients. To test this, we obtained high-resolution resting-state EEG recordings in a population of 20 patients with unilateral ischemic stroke exhibiting various degrees of motor and cognitive deficits. Quantitative scores of motor as well as frontal, left- and right-hemispheric cognitive function were compared to indices of EEG FC of the entire cortex.

## **2. Material and Methods**

### *2.1. Patients and Healthy Control Subjects*

The study was approved by University Hospital of Geneva Ethics Committee. Twenty stroke patients (mean age 61 years, range 37-80, 9 females, see Supplementary Table) and 19 age matched healthy participants (mean age 67 years, range 36-88, 13 females) were included after written informed consent. Ages ( $p=0.16$ , Mann-Whitney U test) and gender ( $p=0.09$ , Fisher's exact test) did not differ significantly between groups. All patients were diagnosed with first-ever unilateral, territorial, ischemic stroke in the territories of the middle and/or anterior cerebral artery and were recorded 3 months post stroke onset. Exclusion criteria were: previous neurological, psychiatric, or cognitive impairment; preexisting brain lesion visible in the CT/MRI on admission (except lacunar lesions or white matter hyperintensities); epileptic seizures; persistent post stroke delirium; ischemic lesions in the brain stem, thalamus, or cerebellum; right hemispheric language dominance; metallic objects in the brain; skull breach; medical complications. The mean National Institute of Health Stroke Scale (NIHSS) was 13 (range 3-27). All patients received standard therapy at the stroke unit during the acute phase and an individually tailored multidisciplinary rehabilitation program in the subacute and chronic phases.

### *2.2. Data acquisition*

EEG was recorded with a 128-channel Biosemi ActiveTwo EEG-system (Biosemi B.V., Amsterdam, Netherlands) at a sampling rate of 512 Hz in an awake, resting condition during which subjects kept their eyes closed. The participants were asked to remain awake, and vigilance was verified in the recorded online EEG. Artifacts and data segments with abundant signs of drowsiness were excluded by visual inspection of the data. Five minutes of artifact-free data were recalculated against the average reference.

### *2.3. Clinical assessments*

Motor function was evaluated in all 20 patients. Grip strength was measured with a Jamar dynamometer (Mathiowetz et al., 1985), dexterity with the Nine Hole Peg test (Oxford et al., 2003), and upper extremity motor function with the upper extremity components of the Stroke Rehabilitation Assessment of Movement (STREAM) (Wang et al., 2002) and the Fugl-Meyer score (Fugl-Meyer et al., 1975). All scores were normalized to unaffected contralateral values of the same

patient. The Nine Hole Peg test was expressed in pegs/sec. Since the 4 motor scores were highly correlated among each other ( $r > .8$ ), they were averaged to a composite motor score.

Verbal attention was quantified with verbal fluency and verbal working memory tasks, and right spatial attention with a spatial working memory task. The verbal fluency described the number of produced words to a given initial letter ('P' or 'M') within two minutes and could be quantified in 14 patients. In the verbal working memory (=digit span) task the patients were asked to repeat a list of numbers in the original and inverse order (Wechsler, 1997). It could be measured in 12 patients. In the spatial working memory (=spatial span) task, patients had to reproduce immediately the sequences of spatially distributed cubes in the original and inverse order (Wechsler, 1997). It was obtained from 10 patients.

#### *2.4. Structural magnetic resonance imaging*

Structural magnetic resonance images were acquired on a Siemens 3.0-Tesla Trio scanner (Siemens Medical Solutions, Erlangen, Germany). The protocol contained a high-resolution T1-weighted, 3-D spoiled gradient-recalled echo in a steady state sequence covering the whole skull for creation of the head models. T2-weighted three-dimensional fast spin-echo, DWI, and FLAIR sequences were used to delineate ischemic lesions in the software MRICro (<http://www.cabiatl.com/mricro/>) written by Chris Rorden.

#### *2.5. Functional connectivity analysis*

Source FC was calculated in Matlab (The MathWorks Inc., Natick, USA) with NUTMEG (<http://nutmeg.berkeley.edu>) (Dalal et al., 2011) and its FCM toolbox (Guggisberg et al., 2011). The detailed analysis steps and their validation have been described previously (Guggisberg et al., 2011; Guggisberg et al., 2008). In short, we computed the lead-potential with 10 mm grid spacing (~800 voxels depending on the patient) using a spherical head model with anatomical constraints (SMAC) (Spinelli et al., 2000) based on the segmented grey matter of the individual T1 MRI. The average referenced EEG was bandpass-filtered between 1 and 20 Hz and non-overlapping data segments of 1 s duration were tapered with a Hanning window and Fourier transformed. Fourier coefficients were then projected to grey matter voxels with an adaptive spatial filter (scalar minimum variance beamformer) (Sekihara et al., 2004). We subsequently calculated the imaginary component of coherence (IC) (Nolte et al., 2004; Sekihara et al., 2011) between all possible voxel pairs during the entire resting-state recording for each frequency bin between 1 and 20 Hz (frequencies <1 Hz and

>20 Hz were not investigated because of the larger susceptibility to artifacts and technological limitations of surface EEG to reliably reconstruct these rhythms). Computation time for all pairwise IC values in one subject was ~20 s on a single standard PC. In order to examine this multi-dimensional data array, we used a two-step approach. First, we calculated the FC of each voxel as the average absolute IC across its connections with all other voxels. Second, we extracted anatomical regions showing largest changes in the first analysis step and calculated the IC between these seed nodes and all other voxels to examine the spatial structure of their functional interactions.

FC maps of each patient were normalized, for each frequency bin, to the mean IC value across all voxels by calculating z-scores. Z-score maps were spatially normalized to the canonical MNI brain space with SPM8 (<http://www.fil.ion.ucl.ac.uk/spm/software/spm8/>). Ischemic lesions were masked during spatial normalization to avoid distortion. FC maps were rendered on a 3D brain with SPM8 and Cartool (<http://sites.google.com/site/cartoolcommunity/home>).

## *2.6. Statistical analyses*

Unpaired *t*-tests were applied to assess differences in power and IC magnitude between patients and controls at the electrode level, paired *t*-tests to assess differences between lesion-side and contralesional electrodes.

IC maps of each patient were compared voxel-wise against the mean of an age matched healthy control population with *t*-tests for one sample, corrected for testing multiple voxels with a 1% false discovery rate.

Scores of motor and cognitive function in patients were correlated with IC at each brain area in order to evaluate the functional and clinical significance of the observed connectivity changes. For correlations with the composite motor score, the maps of patients with right hemispheric lesions were right-left flipped in order to align affected and unaffected sides, in addition to a separate analysis of right and left sided motor deficits. To assess the topography of the correlates of neurological function, correlations were first performed voxel-wise with statistical non-parametric mapping (SnPM), using a cluster correction of the family-wise error (Singh et al., 2003). To further assert that the correlations are functionally and topographically specific, we extracted mean alpha band IC values of 14 anatomical regions of interest (ROIs) in the middle cerebral artery territories using Anatomical Automatic Labeling (AAL) templates (Tzourio-Mazoyer et al., 2002) and correlated them with clinical scores. In order to verify that the associations were not merely due to structural lesions of the ROIs, individual anatomical ROIs were additionally subjected to a partial correlation

analysis with the factor ‘% of ROI affected by lesion’ as covariate. A logistic regression was performed to assess the sensitivity and specificity of ROI IC for separating patients with below average performance in a given function from patients with above average performance using published average test scores of healthy populations (Mathiowetz et al., 1985; Oxford et al., 2003; Wechsler, 1997) as cutoff to dichotomize clinical scores.

### 3. Results

The lesion distribution of the 20 patients analyzed in this study is depicted in Figure 1. The territories of the middle cerebral arteries were most frequently affected.

Power and IC changes in affected hemispheres of stroke patients could be observed already at the electrode level (Fig. 2). Brain lesions induced a shift from fast to slow rhythms with increased delta (1-3 Hz,  $p < 0.003$ ) and theta power (4-7 Hz,  $p < 0.014$ ) but decreased beta power (13-20 Hz,  $p < 0.031$ ). Overall alpha power (8-12 Hz) did not change significantly ( $p > 0.69$ ), but the alpha power peak frequency decreased from 9.2 Hz in healthy subjects to 8.5 Hz in patients ( $p = 0.043$ ). Conversely, mean absolute IC between the ipsilesional central electrode (C3 or C4) and all other electrodes was significantly decreased in the alpha band ( $p < 0.023$ ) and increased in the delta band ( $p < 0.022$ ).

These spectral IC changes were then localized with an adaptive spatial filter. Figure 3 shows cortical IC changes in two patients with ischemic stroke in the territory of the left middle cerebral artery compared to a healthy control population. The maps show the network nodes that are most affected in each patient. They depict the average absolute IC of each voxel across its connections with all other cortical voxels, contrasted to the average map of all healthy subjects (A-B). The clinical picture three months after stroke was dominated by a severe non-fluent aphasia in patient AZ, whereas patient PD demonstrated a severe paresis of the right arm (C-D). The FC maps show corresponding local IC decreases between network nodes that are known to participate in the affected functions and the rest of the brain: the left fronto-temporal cortex for subject AZ and the left motor/premotor cortex in subject PD (marked in blue in Fig. 3 A-B). This IC decrease concerned most prominently EEG oscillations in the alpha frequency range (7-13 Hz) for both patients (E-F). It is not always part of an ischemic lesion, and only some of the functional connections between blue regions and other brain regions were decreased, whereas others were comparable to or even greater than in the control population (G-H).

We then asked whether local IC changes are linearly related to motor and cognitive function of the patients. Figure 4 illustrates the Pearson correlation analysis in the patients between the clinical

performance after stroke and the mean resting-state IC at each voxel. Good performance in the verbal fluency and verbal working memory tasks correlated with higher IC between the left fronto-opercular cortex and the rest of the brain. Similarly, the composite motor score correlated with IC in the contralateral motor cortex, and spatial working memory performance with IC in the right inferior parietal cortex. Correlations between alpha IC and behavior therefore yielded maps of the function of the entire cortex in accordance with the functional specialization known from activation and lesion studies [e.g., (Glascher et al., 2009)]. Moreover, significant negative correlations were observed between behavioral scores and IC in brain regions contralateral to the positive correlations. All these correlations were specific to IC in the alpha frequency band, and could not be observed in other oscillation frequencies. They remained significant and essentially unchanged in topography and frequency distribution when adjusting for age and lesion size with partial correlations (Supplementary Fig. 1).

The analysis of IC in anatomical regions of interest (ROIs) confirmed the functional specificity of the observed correlations (Fig. 5). Alpha band IC between each ROI and the rest of the brain correlated only with functionally related, but not with unrelated clinical scores. The performance of the patients in the verbal fluency and verbal working memory task correlated positively with IC in the left inferior IFG ( $r \geq .85$ ,  $p \leq .0009$ ) and middle frontal gyrus (MFG,  $r \geq .72$ ,  $p \leq .012$ ) and negatively in the right IFG ( $r \leq -.64$ ,  $p \leq .014$ ) and MFG ( $r \leq -.54$ ,  $p \leq .044$ ). Spatial working memory performance showed positive correlations with IC in the right inferior parietal lobule (IPL,  $r = .66$ ,  $p = .040$ ) and negative correlations with IC in the left IPL ( $r = -.91$ ,  $p = .0003$ ) and left superior parietal lobule (SPL,  $r = -.84$ ,  $p = .003$ ). Significant positive correlations were also observed between the composite motor score and IC in the affected precentral gyrus (PCG,  $r = .57$ ,  $p = .009$ ). A partial correlation analysis confirmed that these associations could not be explained by the percentage of the ROI affected by structural lesions (left IFG:  $r \geq .68$ ,  $p \leq 0.029$ ; right IPL:  $r = .69$ ,  $p = .04$ ; affected PCG:  $r = .55$ ,  $p = .016$ ). The logistic regression analysis revealed that IC in the left IFG predicted below-average verbal fluency and verbal working memory performance ( $z\text{-score} < 0$ ) in this small dataset with a sensitivity and specificity of 100% each. The sensitivity and specificity of IC in the right IPL for predicting below-average spatial working memory performance was also 100%. IC in the affected PCG predicted a composite motor score of  $< 90\%$  of maximum score in the affected arm with a sensitivity of 84% and a specificity of 100%.

Next, we explored the spatial structure of alpha coherence networks. In Figure 6, we assess, for nodes showing high overall correlation with behavior in the analyses above, which of the functional connections to the rest of the brain were behaviorally most relevant. When the left IFG was set as seed region, alpha band IC with the left superior temporal lobe, the left temporo-parietal junction, and bilateral associative occipital cortex showed highest correlations with verbal fluency/working

memory performance. For the right IPL, IC to the right middle frontal gyrus (MFG) was most correlated with spatial working memory performance. Composite motor score performance correlated most with IC between the two primary motor cortices.

## **4. Discussion**

This study is the first to reveal the electrical network correlates of neurological deficits. It demonstrates that a disruption of coherent electrical oscillations at rest is linearly correlated with neurological deficits. A stroke-induced decrease in alpha band coherence between a given node and the rest of the brain is highly predictive of deficits in the function of the node, independent of anatomical lesions in this area. We therefore confirm previous fMRI reports of a linear association between synchronous blood-oxygen fluctuations and performance (Carter et al., 2010; He et al., 2007; Koyama et al., 2011; Wang et al., 2010) and extend them to actual neural oscillations in typical EEG frequencies. Thereby, we observe a selective frequency distribution of behaviorally relevant FC changes. IC in dysfunctional brain areas was reduced most consistently in the alpha frequency band and alpha band FC but not FC in other traditional EEG frequencies correlated with cognitive and motor function. Hence, alpha oscillation synchrony is a specific electrical biomarker of neurological function in patients with brain lesions, which allows mapping the functionality as well as the network organization of the entire cortex by means of a single resting-state EEG recording. The results also add to our understanding of the functional relevance of alpha oscillations, which represent the most prominent feature of the human awake resting-state EEG.

### *4.1. Resting-state marker of behaviorally relevant network interactions*

It is important to note that although we correlate brain regions with behavior in a similar way as it is done in traditional lesion studies, the FC measure does not retrace structural lesions but captures changes in network synchrony. The following observations strongly suggest that the reported decreases in alpha band IC do not result from absence of neural tissue generating alpha oscillations but from behaviorally relevant disruptions of network interactions.

First, reduced IC did not only occur within the boundaries of the ischemic lesions, but also at distant and even contralateral nodes. In turn, some parts of the structural lesion did not show decreased alpha band IC (Fig. 3).

Second, partial correlations confirmed that the linear relationship between alpha band IC and behavioral performance is independent of the size and topography of anatomical lesions.

Third, maps did not only show IC decreases but also regions with increased IC. This would not be expected in case of a mere absence of neural tissue, but indeed corresponds to network effects of brain lesions as they were predicted by modeling studies (Alstott et al., 2009). The significance of these increases is largely unknown and needs to be examined in future studies.

Fourth, IC disruptions did not concern all connections of a given node, as would be expected in case of a local lesion effect, but were selective in each patient in accordance with the clinical deficits. For instance, patient AZ with Broca's aphasia suffered from significant functional disconnections between the left IFG and left parietal regions whereas its connections to other areas were preserved or even increased (Fig. 3, G-H).

Fifth, IC disruptions did not concern all oscillation frequencies, as would be expected in case of absence of neural tissue, but selectively the alpha frequency band (Figs. 2 B and 3 E-F).

The ability of alpha band IC to capture behaviorally relevant changes in network function enables excellent sensitivities and specificities close to 100% for separating between deficits and normal function, which might be difficult to achieve with lesion maps that are blind to distant network effects.

#### *4.2. The role of alpha oscillation synchrony after stroke*

In order to ensure that the correlation of alpha band IC with neurological function is not confounded by methodological issues, we performed several additional tests.

- (i) In order to verify that the inverse solution applied in this study did not modify the frequency distribution of the observed FC changes, we calculated IC changes also between electrodes. IC between the central electrode of the affected hemisphere (C3 or C4) and all other electrodes was reduced most consistently in the alpha band as compared to the central electrode of the unaffected hemisphere or to healthy controls (Fig. 2 B), thus reproducing the observations at the voxel level (Fig. 3 E-F). Note however, that alpha band coherence at central electrodes did not correlate with motor function ( $|r| < 0.25$ ,  $p > 0.28$ ), probably because it reflects neural activity not only from the motor cortex but from wide-spread brain regions (Schoffelen and Gross, 2009).
- (ii) In the analyses reported above, we quantified FC between brain regions with the imaginary component of coherence (Nolte et al., 2004), which, unlike magnitude squared coherence, is robust to overestimations and distortions of cortical connectivity due to spatial leakage of the

inverse solutions (Guggisberg et al., 2008; Sekihara et al., 2011). However, IC only captures functional interactions occurring with some time delay and discards zero-lag synchrony. Hence, its magnitude depends not only on the strength of coupling but also on the phase delay, which might have influenced our results. We therefore additionally correlated maps of magnitude squared coherence with motor and cognitive scores of the patients while controlling for spatial leakage by other means (see Supplementary Methods). This reproduced essentially the same findings as when using IC; correlations with neurological function were again specific to the alpha frequency band (Supplementary Fig. 2).

- (iii) Coherence is not a pure measure of phase synchrony but is additionally influenced by the amplitude of signals. Our comparison of the clinical relevance of different EEG frequencies might therefore merely reflect the higher amplitude of alpha activity in the resting EEG. However, Figure 2 shows a decrease of alpha IC in stroke hemispheres without corresponding change in alpha power. In order to further exclude this possibility, we additionally correlated relative alpha power at each voxel with clinical scores of the patients and could not find any significantly correlated region ( $p > 0.05$ , cluster corrected). Furthermore, we quantified the FC at each brain voxel with an amplitude-independent measure of phase synchrony: the phase lag index (Stam et al., 2007). Again, correlations between clinical performance and the phase lag index could only be observed in the alpha frequency band (Supplementary Fig. 3).

The observed relationship between alpha band IC and behavior is therefore robust to different measures of FC and due to oscillation synchrony rather than to amplitude. We can thus conclude that the stroke-induced disruption of resting-state alpha band coherence and phase synchrony is closely associated with neurological deficits. Conversely, the lack of correlation of other frequency bands with patient performance in our analyses may be due to several factors and must not be interpreted as absence of behavioral relevance of coherence in these bands. For instance, all measures of FC are sensitive to noise and the alpha band tends to have a greater signal-to-noise ratio, especially compared to faster rhythms. Furthermore, our analyses were restricted to the resting-state whereas other EEG frequencies may be more implicated during tasks (Gerloff et al., 2006).

The functional significance of alpha rhythms has intrigued researchers already since the first recording of human EEG (Berger, 1929). Alpha power usually decreases during tasks and increases at rest and has therefore been proposed to reflect the inhibition of task-irrelevant cortical areas (Pfurtscheller, 1992). However, numerous previous studies have also observed *increased* alpha rhythms, in particular increased alpha band phase synchrony, during internal tasks, working memory, and attention (Cooper et al., 2003; Jensen et al., 2002; Kolev et al., 2001). Moreover, phase locking in the alpha band predicted behavioral performance for perceptual discrimination (Haegens et al.,

2011; Hanslmayr et al., 2005), conscious perception (Mima et al., 2001; Palva et al., 2005b), and long-term memory formation (Meeuwissen et al., 2011). Rhythmic transcranial magnetic stimulation (TMS) with alpha frequencies but not with other frequencies modulated visual perception (Romei et al., 2010). Taken together, these findings provide evidence for an active role of alpha oscillation synchrony (Palva and Palva, 2007), and our findings strengthen this notion by showing that its disruption is associated with neurological deficits. Previous studies have also observed behaviorally relevant reductions of alpha band FC in patients with tumors (Guggisberg et al., 2008; Martino et al., 2011) and schizophrenia (Haenschel et al., 2010; Hinkley et al., 2011), thus suggesting that the finding is not unique to stroke but a general feature of the resting brain.

Studies examining cross-frequency phase and power relationships have provided insights into how alpha rhythms might achieve their behavioral relevance. Gamma power (>30 Hz), which is thought to reflect neural computation (Crone et al., 1998), is phase-locked to alpha oscillations (Osipova et al., 2008; Palva et al., 2005a). Alpha rhythms therefore seem to synchronize and structure processing in distributed networks by gating the timing of higher frequency oscillations.

#### *4.3. Spatial structure of alpha coherence networks and comparison to fMRI networks*

When investigating the spatial distribution of functionally relevant interactions (Fig. 6), we observed overlaps with previous fMRI descriptions of the topography of resting-state networks associated with language, spatial attention, and motor function (Damoiseaux et al., 2006; Kelly et al., 2010).

Furthermore, we additionally reconstructed networks based on EEG alpha oscillation synchrony in healthy participants of this study and again obtained a similar topography (Supplementary Fig. 4). Hence, alpha coherence seems to follow a similar spatial structure as the much slower synchronous fMRI resting-state networks, which is in accordance with previous observations (Jann et al., 2009).

Despite the similar spatial structure, our results obtained with EEG are quite different to previous fMRI reports of resting-state network changes after stroke. In fMRI analyses, only connections within functional networks, and in particular interhemispheric connections among homologous brain areas, were correlated with performance (Carter et al., 2010; He et al., 2007). Conversely, functionally relevant interactions were obtained when assessing connections to the entire cortex of each region in our EEG study. Moreover, a previous MEG study observed the best topographical match between MEG and fMRI networks for amplitude envelope correlations in beta-frequency band (Brookes et al., 2011b) which differs from the alpha band coherence and phase synchrony found to be most closely associated with behavior in this study. Future direct comparisons of fMRI and EEG/MEG networks

will need to investigate whether these dissimilarities represent different network systems or methodological differences in assessing neurological function and network structure.

#### *4.4. Alpha band FC captures misbalance in interhemispheric inhibition*

The more diffuse representation of functionally relevant interactions in EEG analyses may also have advantages, as it enabled us to observe, for all functions, opposite correlations between alpha band FC and clinical data among homologous areas of both hemispheres, which has not been reported in fMRI studies. For instance, we observed significant *negative* correlations between verbal fluency/working memory performance and FC in the right IFG, which contrasts with the *positive* correlations of its left counterpart. Hence, larger alpha synchrony in the right IFG was associated with poorer verbal fluency/working memory. This negative correlation may correspond to a dysbalance in mutual interhemispheric inhibition which is well-known from functional imaging (Cao et al., 1999; Corbetta et al., 2005) and TMS studies (Murase et al., 2004; Naeser et al., 2005; Nyffeler et al., 2009; Weiduschat et al., 2011). According to this concept, the two hemispheres normally maintain a dynamic balance by competitively inhibiting each other during activation. Unilateral brain lesions lead to reduced inhibitory afferences from the lesion and hence to an abnormal hyperactivity of the unaffected hemisphere, which in turn further inhibits the perilesional tissue (Cao et al., 1999; Murase et al., 2004). Contralesional hyperactivity is therefore indeed negatively related to performance as we observe it in our maps. Our results suggest that it is associated with a relative hypersynchrony in alpha oscillations.

To our knowledge, this is the only technique that can scan the entire cortex for lesion-induced dysbalance in inter-hemispheric inhibition. It may prove useful for accompanying brain stimulation therapies trying to restore the balance.

#### *4.5. Clinical applications*

The ability of a single resting-state EEG recording to capture the network basis of cognitive and motor deficits in patients as well as changes in the neural network organization offers exciting new perspectives for research and clinical practice. For instance, this technique may contribute to the understanding of neuronal plasticity of the brain. The low costs and ubiquitous availability of EEG, the ease of obtaining resting-state recordings even in severely affected patients, and the excellent sensitivity and specificity of the measure for predicting neurological function make this approach

highly suitable for applications in therapy and rehabilitation, e.g., to obtain information on the individual neural state of the patients.

## 5. Acknowledgments

This work was supported by the Swiss National Science Foundation (grant number 320030\_129679). Cartool is programmed by Denis Brunet and supported by the Center for Biomedical Imaging (CIBM). We would like to thank the anonymous reviewers for helpful comments.

## 6. References

- Alstott, J., Breakspear, M., Hagmann, P., Cammoun, L., Sporns, O., 2009. Modeling the impact of lesions in the human brain. *PLoS Comput Biol* 5, e1000408.
- Berger, H., 1929. Über das elektroenkephalogramm des menschen. *Arch. Psychiat. NervKrankh.* 87, 527-570.
- Britz, J., Van De Ville, D., Michel, C.M., 2010. Bold correlates of eeg topography reveal rapid resting-state network dynamics. *Neuroimage* 52, 1162-1170.
- Brookes, M.J., Hale, J.R., Zumer, J.M., Stevenson, C.M., Francis, S.T., Barnes, G.R., Owen, J.P., Morris, P.G., Nagarajan, S.S., 2011a. Measuring functional connectivity using meg: Methodology and comparison with fcmri. *Neuroimage* 56, 1082-1104.
- Brookes, M.J., Woolrich, M., Luckhoo, H., Price, D., Hale, J.R., Stephenson, M.C., Barnes, G.R., Smith, S.M., Morris, P.G., 2011b. Investigating the electrophysiological basis of resting state networks using magnetoencephalography. *Proc Natl Acad Sci U S A* 108, 16783-16788.
- Cao, Y., Vikingstad, E.M., George, K.P., Johnson, A.F., Welch, K.M., 1999. Cortical language activation in stroke patients recovering from aphasia with functional mri. *Stroke* 30, 2331-2340.
- Carter, A.R., Astafiev, S.V., Lang, C.E., Connor, L.T., Rengachary, J., Strube, M.J., Pope, D.L., Shulman, G.L., Corbetta, M., 2010. Resting interhemispheric functional magnetic resonance imaging connectivity predicts performance after stroke. *Ann. Neurol.* 67, 365-375.
- Cooper, N.R., Croft, R.J., Dominey, S.J., Burgess, A.P., Gruzeliier, J.H., 2003. Paradox lost? Exploring the role of alpha oscillations during externally vs. Internally directed attention and the implications for idling and inhibition hypotheses. *Int J Psychophysiol* 47, 65-74.
- Corbetta, M., Kincade, M.J., Lewis, C., Snyder, A.Z., Sapir, A., 2005. Neural basis and recovery of spatial attention deficits in spatial neglect. *Nat Neurosci* 8, 1603-1610.
- Cramer, S.C., 2008. Repairing the human brain after stroke: I. Mechanisms of spontaneous recovery. *Ann.Neurol.* 63, 272-287.
- Crone, N.E., Miglioretti, D.L., Gordon, B., Lesser, R.P., 1998. Functional mapping of human sensorimotor cortex with electrocorticographic spectral analysis. Ii. Event-related synchronization in the gamma band. *Brain* 121, 2301-2315.
- Dalal, S.S., Zumer, J.M., Guggisberg, A.G., Trumpis, M., Wong, D.D., Sekihara, K., Nagarajan, S.S., 2011. Meg/eeg source reconstruction, statistical evaluation, and visualization with nutmeg. *Comput Intell Neurosci* 2011, 758973.
- Damoiseaux, J.S., Rombouts, S.A., Barkhof, F., Scheltens, P., Stam, C.J., Smith, S.M., Beckmann, C.F., 2006. Consistent resting-state networks across healthy subjects. *Proc Natl Acad Sci U S A* 103, 13848-13853.
- de Pasquale, F., Della Penna, S., Snyder, A.Z., Lewis, C., Mantini, D., Marzetti, L., Belardinelli, P., Ciancetta, L., Pizzella, V., Romani, G.L., Corbetta, M., 2010. Temporal dynamics of spontaneous meg activity in brain networks. *Proc Natl Acad Sci U S A* 107, 6040-6045.
- Fox, M.D., Snyder, A.Z., Vincent, J.L., Corbetta, M., Van, E.D.C., Raichle, M.E., 2005. The human brain is intrinsically organized into dynamic, anticorrelated functional networks. *Proc Natl Acad Sci U.S.A* 102, 9673-9678.
- Fugl-Meyer, A.R., Jaasko, L., Leyman, I., Olsson, S., Steglind, S., 1975. The post-stroke hemiplegic patient. 1. A method for evaluation of physical performance. *Scand. J. Rehabil. Med.* 7, 13-31.

- Gerloff, C., Bushara, K., Sailer, A., Wassermann, E.M., Chen, R., Matsuoka, T., Waldvogel, D., Wittenberg, G.F., Ishii, K., Cohen, L.G., Hallett, M., 2006. Multimodal imaging of brain reorganization in motor areas of the contralesional hemisphere of well recovered patients after capsular stroke. *Brain* 129, 791-808.
- Glascher, J., Tranel, D., Paul, L.K., Rudrauf, D., Rorden, C., Hornaday, A., Grabowski, T., Damasio, H., Adolphs, R., 2009. Lesion mapping of cognitive abilities linked to intelligence. *Neuron* 61, 681-691.
- Greicius, M.D., Krasnow, B., Reiss, A.L., Menon, V., 2003. Functional connectivity in the resting brain: A network analysis of the default mode hypothesis. *Proc Natl Acad Sci U S A* 100, 253-258.
- Gross, J., Kujala, J., Hamalainen, M., Timmermann, L., Schnitzler, A., Salmelin, R., 2001. Dynamic imaging of coherent sources: Studying neural interactions in the human brain. *Proc Natl Acad Sci U.S.A* 98, 694-699.
- Guggisberg, A.G., Dalal, S.S., Zumer, J.M., Wong, D.D., Dubovik, S., Michel, C.M., Schnider, A., 2011. Localization of cortico-peripheral coherence with electroencephalography. *Neuroimage* 57, 1348-1357.
- Guggisberg, A.G., Honma, S.M., Findlay, A.M., Dalal, S.S., Kirsch, H.E., Berger, M.S., Nagarajan, S.S., 2008. Mapping functional connectivity in patients with brain lesions. *Ann. Neurol.* 63, 193-203.
- Haegens, S., Handel, B.F., Jensen, O., 2011. Top-down controlled alpha band activity in somatosensory areas determines behavioral performance in a discrimination task. *J Neurosci* 31, 5197-5204.
- Haenschel, C., Linden, D.E., Bittner, R.A., Singer, W., Hanslmayr, S., 2010. Alpha phase locking predicts residual working memory performance in schizophrenia. *Biol Psychiatry* 68, 595-598.
- Hanslmayr, S., Klimesch, W., Sauseng, P., Gruber, W., Doppelmayr, M., Freunberger, R., Pecherstorfer, T., 2005. Visual discrimination performance is related to decreased alpha amplitude but increased phase locking. *Neurosci Lett* 375, 64-68.
- He, B.J., Raichle, M.E., 2009. The fmri signal, slow cortical potential and consciousness. *Trends Cogn Sci* 13, 302-309.
- He, B.J., Snyder, A.Z., Vincent, J.L., Epstein, A., Shulman, G.L., Corbetta, M., 2007. Breakdown of functional connectivity in frontoparietal networks underlies behavioral deficits in spatial neglect. *Neuron* 53, 905-918.
- He, B.J., Snyder, A.Z., Zempel, J.M., Smyth, M.D., Raichle, M.E., 2008. Electrophysiological correlates of the brain's intrinsic large-scale functional architecture. *Proc Natl Acad Sci U S A* 105, 16039-16044.
- He, B.J., Zempel, J.M., Snyder, A.Z., Raichle, M.E., 2010. The temporal structures and functional significance of scale-free brain activity. *Neuron* 66, 353-369.
- Hinkley, L.B., Vinogradov, S., Guggisberg, A.G., Fisher, M., Findlay, A.M., Nagarajan, S.S., 2011. Clinical symptoms and alpha band resting-state functional connectivity imaging in patients with schizophrenia: Implications for novel approaches to treatment. *Biol Psychiatry* 70, 1134-1142.
- Honey, C.J., Sporns, O., 2008. Dynamical consequences of lesions in cortical networks. *Hum. Brain Mapp.* 29, 802-809.
- Jann, K., Dierks, T., Boesch, C., Kottlow, M., Strik, W., Koenig, T., 2009. Bold correlates of eeg alpha phase-locking and the fmri default mode network. *Neuroimage* 45, 903-916.
- Jensen, O., Gelfand, J., Kounios, J., Lisman, J.E., 2002. Oscillations in the alpha band (9-12 hz) increase with memory load during retention in a short-term memory task. *Cereb Cortex* 12, 877-882.
- Kelly, C., Uddin, L.Q., Shehzad, Z., Margulies, D.S., Castellanos, F.X., Milham, M.P., Petrides, M., 2010. Broca's region: Linking human brain functional connectivity data and non-human primate tracing anatomy studies. *Eur J Neurosci* 32, 383-398.
- Kolev, V., Yordanova, J., Schurmann, M., Basar, E., 2001. Increased frontal phase-locking of event-related alpha oscillations during task processing. *Int J Psychophysiol* 39, 159-165.
- Koyama, M.S., Di Martino, A., Zuo, X.N., Kelly, C., Mennes, M., Jutagir, D.R., Castellanos, F.X., Milham, M.P., 2011. Resting-state functional connectivity indexes reading competence in children and adults. *J Neurosci* 31, 8617-8624.
- Martino, J., Honma, S.M., Findlay, A.M., Guggisberg, A.G., Owen, J.P., Kirsch, H.E., Berger, M.S., Nagarajan, S.S., 2011. Resting functional connectivity in patients with brain tumors in eloquent areas. *Ann Neurol* 69, 521-532.
- Mathiowetz, V., Kashman, N., Volland, G., Weber, K., Dowe, M., Rogers, S., 1985. Grip and pinch strength: Normative data for adults. *Arch. Phys. Med. Rehabil.* 66, 69-74.
- Meeuwissen, E.B., Takashima, A., Fernandez, G., Jensen, O., 2011. Increase in posterior alpha activity during rehearsal predicts successful long-term memory formation of word sequences. *Hum Brain Mapp* 32, 2045-2053.
- Mima, T., Oluwatimilehin, T., Hiraoka, T., Hallett, M., 2001. Transient interhemispheric neuronal synchrony correlates with object recognition. *J Neurosci* 21, 3942-3948.
- Monto, S., Palva, S., Voipio, J., Palva, J.M., 2008. Very slow eeg fluctuations predict the dynamics of stimulus detection and oscillation amplitudes in humans. *J Neurosci* 28, 8268-8272.

- Murase, N., Duque, J., Mazzocchio, R., Cohen, L.G., 2004. Influence of interhemispheric interactions on motor function in chronic stroke. *Ann Neurol* 55, 400-409.
- Musso, F., Brinkmeyer, J., Mobascher, A., Warbrick, T., Winterer, G., 2010. Spontaneous brain activity and eeg microstates. A novel eeg/fmri analysis approach to explore resting-state networks. *Neuroimage* 52, 1149-1161.
- Naeser, M.A., Martin, P.I., Nicholas, M., Baker, E.H., Seekins, H., Kobayashi, M., Theoret, H., Fregni, F., Maria-Tormos, J., Kurland, J., Doron, K.W., Pascual-Leone, A., 2005. Improved picture naming in chronic aphasia after tms to part of right broca's area: An open-protocol study. *Brain Lang* 93, 95-105.
- Nolte, G., Bai, O., Wheaton, L., Mari, Z., Vorbach, S., Hallett, M., 2004. Identifying true brain interaction from eeg data using the imaginary part of coherency. *Clin. Neurophysiol.* 115, 2292-2307.
- Nyffeler, T., Cazzoli, D., Hess, C.W., Muri, R.M., 2009. One session of repeated parietal theta burst stimulation trains induces long-lasting improvement of visual neglect. *Stroke* 40, 2791-2796.
- Osipova, D., Hermes, D., Jensen, O., 2008. Gamma power is phase-locked to posterior alpha activity. *PLoS One* 3, e3990.
- Oxford, G.K., Vogel, K.A., Le, V., Mitchell, A., Muniz, S., Vollmer, M.A., 2003. Adult norms for a commercially available nine hole peg test for finger dexterity. *Am. J. Occup. Ther.* 57, 570-573.
- Palva, J.M., Palva, S., Kaila, K., 2005a. Phase synchrony among neuronal oscillations in the human cortex. *J Neurosci* 25, 3962-3972.
- Palva, S., Linkenkaer-Hansen, K., Naatanen, R., Palva, J.M., 2005b. Early neural correlates of conscious somatosensory perception. *J Neurosci* 25, 5248-5258.
- Palva, S., Palva, J.M., 2007. New vistas for alpha-frequency band oscillations. *Trends Neurosci* 30, 150-158.
- Pfurtscheller, G., 1992. Event-related synchronization (ers): An electrophysiological correlate of cortical areas at rest. *Electroencephalogr. Clin. Neurophysiol.* 83, 62-69.
- Raichle, M.E., 2011. The restless brain. *Brain Connectivity* 1, 3-12.
- Romei, V., Gross, J., Thut, G., 2010. On the role of prestimulus alpha rhythms over occipito-parietal areas in visual input regulation: Correlation or causation? *J Neurosci* 30, 8692-8697.
- Schoffelen, J.M., Gross, J., 2009. Source connectivity analysis with meg and eeg. *Hum Brain Mapp* 30, 1857-1865.
- Schoffelen, J.M., Oostenveld, R., Fries, P., 2008. Imaging the human motor system's beta-band synchronization during isometric contraction. *Neuroimage* 41, 437-447.
- Sekihara, K., Nagarajan, S.S., Poeppel, D., Marantz, A., 2004. Asymptotic snr of scalar and vector minimum-variance beamformers for neuromagnetic source reconstruction. *IEEE Trans Biomed Eng* 51, 1726-1734.
- Sekihara, K., Owen, J.P., Trisno, S., Nagarajan, S.S., 2011. Removal of spurious coherence in meg source-space coherence analysis. *IEEE Trans Biomed Eng* 58, 3121-3129.
- Singh, K.D., Barnes, G.R., Hillebrand, A., 2003. Group imaging of task-related changes in cortical synchronisation using nonparametric permutation testing. *Neuroimage* 19, 1589-1601.
- Spinelli, L., Andino, S.G., Lantz, G., Seeck, M., Michel, C.M., 2000. Electromagnetic inverse solutions in anatomically constrained spherical head models. *Brain Topogr* 13, 115-125.
- Stam, C.J., Nolte, G., Daffertshofer, A., 2007. Phase lag index: Assessment of functional connectivity from multi channel eeg and meg with diminished bias from common sources. *Hum Brain Mapp* 28, 1178-1193.
- Tzourio-Mazoyer, N., Landeau, B., Papathanassiou, D., Crivello, F., Etard, O., Delcroix, N., Mazoyer, B., Joliot, M., 2002. Automated anatomical labeling of activations in spm using a macroscopic anatomical parcellation of the mni mri single-subject brain. *Neuroimage* 15, 273-289.
- Van de Ville, D., Britz, J., Michel, C.M., 2010. Eeg microstate sequences in healthy humans at rest reveal scale-free dynamics. *Proc Natl Acad Sci U S A* 107, 18179-18184.
- Vincent, J.L., Patel, G.H., Fox, M.D., Snyder, A.Z., Baker, J.T., Van Essen, D.C., Zempel, J.M., Snyder, L.H., Corbetta, M., Raichle, M.E., 2007. Intrinsic functional architecture in the anaesthetized monkey brain. *Nature* 447, 83-86.
- Wang, C.H., Hsieh, C.L., Dai, M.H., Chen, C.H., Lai, Y.F., 2002. Inter-rater reliability and validity of the stroke rehabilitation assessment of movement (stream) instrument. *J. Rehabil. Med.* 34, 20-24.
- Wang, L., Negreira, A., LaViolette, P., Bakkour, A., Sperling, R.A., Dickerson, B.C., 2010. Intrinsic interhemispheric hippocampal functional connectivity predicts individual differences in memory performance ability. *Hippocampus* 20, 345-351.
- Wechsler, D., 1997. Wechsler memory scale - third edition The Psychological Corporation, San Antonio.
- Weiduschat, N., Thiel, A., Rubi-Fessen, I., Hartmann, A., Kessler, J., Merl, P., Kracht, L., Rommel, T., Heiss, W.D., 2011. Effects of repetitive transcranial magnetic stimulation in aphasic stroke: A randomized controlled pilot study. *Stroke* 42, 409-415.

Weiller, C., Ramsay, S.C., Wise, R.J., Friston, K.J., Frackowiak, R.S., 1993. Individual patterns of functional reorganization in the human cerebral cortex after capsular infarction. *Ann. Neurol.* 33, 181-189.

Zhao, J., Liu, J., Li, J., Liang, J., Feng, L., Ai, L., Lee, K., Tian, J., 2011. Intrinsically organized network for word processing during the resting state. *Neurosci Lett* 487, 27-31.

## 7. Figure Legends

### Figure 1. Lesion distribution of the 20 patients with ischemic stroke included in the study.

The color encodes the number of patients with ischemic lesion at a given voxel. The territories of the middle cerebral arteries were most frequently and more or less symmetrically affected.

### Figure 2. Spectrogram of power and imaginary coherence at the electrode level.

**A** Mean power spectrum across electrodes ( $\pm$  standard error of mean) showing shift from fast to slow rhythms in stroke patients. **B** Mean IC ( $\pm$  standard error of mean) between the central electrode (C3/C4) of the affected hemisphere and all other electrodes was selectively reduced in the alpha frequency range (8-12 Hz) as compared to IC between the central electrode of the unaffected hemisphere ( $p=0.0018$ , paired  $t$ -test) or to IC of healthy controls ( $p=0.023$ , unpaired  $t$ -test).

### Figure 3. Example of resting-state functional connectivity maps in 2 patients with ischemic stroke in the territory of the left middle cerebral artery.

**A, B** The ischemic lesion is marked in *dark grey*. Nodes showing significant decreases in FC with the rest of the brain as compared to a healthy control population are marked in *blue*, significant relative increases in *red* ( $p<0.05$ , corrected with 1% FDR). The topography of disconnected nodes reflects the profile of neurological deficits of each patient (**C, D**). **E, F** FC reductions in affected areas (*blue lines*) as compared to the mean ( $\pm$  SD) of the entire cortex of each patient (*grey lines*) were most prominent in the alpha frequency range (7-13 Hz). **G, H** FC of primarily affected nodes in patients (*black bars*) as compared to the mean ( $\pm$  SD) of healthy controls (*white bars*). Only selected connections of each node were disrupted whereas other connections were preserved or even increased (\*  $p<0.05$ , \*\*  $p<0.01$ , \*\*\*  $p<0.001$ ). *Abbreviations:* IC, imaginary coherence; FC, functional connectivity; L, left; R, right; IFG, inferior frontal gyrus; MFG, middle frontal gyrus; PCG, precentral gyrus; IPL, inferior parietal lobule; SPL, superior parietal lobule; STG, superior temporal gyrus; MTG, middle temporal gyrus.

**Figure 4. Voxel-wise linear correlation of resting-state functional connectivity of the patients with their performance in functional tests.**

Significant positive correlations (marked in *red*,  $p < 0.05$ , cluster corrected) could be observed only in nodes known to be involved in the processing of the tested function (e.g., in the left inferior frontal gyrus around Broca's area for verbal fluency and verbal working memory). These positive correlations were unique to the alpha frequency band (right column). Conversely, significant negative correlations (*blue*) with alpha band synchrony were found in the contralateral homologous counterparts (e.g., the right inferior frontal gyrus for verbal fluency/verbal working memory), which may be related to a reduction of interhemispheric inhibitory influences from the stroke-affected hemisphere. For correlations with the composite motor score, the maps of patients with right hemispheric lesions were flipped in order to align affected and unaffected sides, in addition to a separate analysis of right and left sided motor function of all patients.

**Figure 5. Connectivity correlates of neurological function in anatomical ROIs within the vascular territory of the middle cerebral artery.**

Significant correlations between neurological function and alpha band FC (marked in red and with asterisks, \*  $p < 0.05$ , \*\*  $p < 0.01$ , \*\*\*  $p < 0.001$ ) could be observed only in functionally related, but not in unrelated ROIs.

*Abbreviations:* L, left; R, right; IFG, inferior frontal gyrus; MFG, middle frontal gyrus; PCG, precentral gyrus; aff, affected; contra, contralateral; IPL, inferior parietal lobule; SPL, superior parietal lobule; STG, superior temporal gyrus; MTG, middle temporal gyrus.

**Figure 6. Topography of the behaviorally most relevant interactions with seed nodes showing high overall correlations with patient performance.**

Alpha band FC between seed nodes (marked *in green*) and the rest of the brain was correlated with behavioral scores; regions with significant positive correlations ( $p < 0.05$ , cluster corrected) are shown *in red*. The topography of functionally meaningful alpha-band interactions overlaps with previous fMRI descriptions of resting-state networks (Damoiseaux et al., 2006; Kelly et al., 2010) and with synchronous alpha-band networks observed in the healthy participants of this study (see Supplementary Figure 4). For correlations with motor function of the affected arm, all lesions were aligned to the left hemisphere.

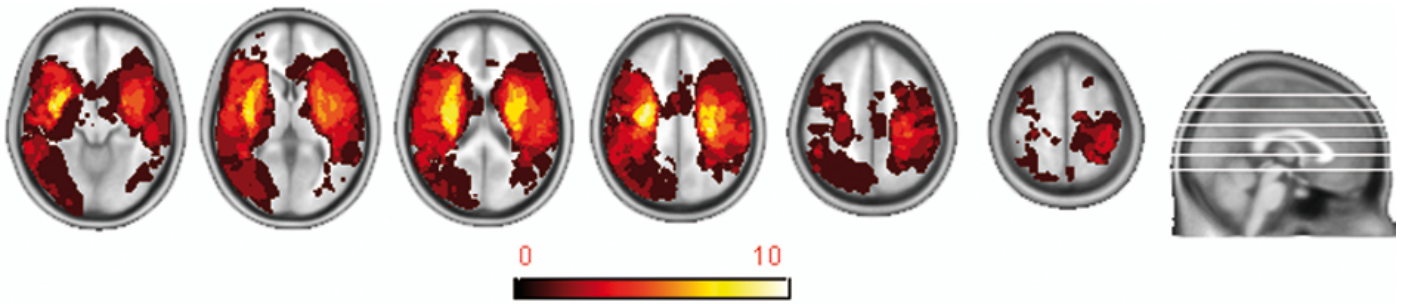


Figure 1

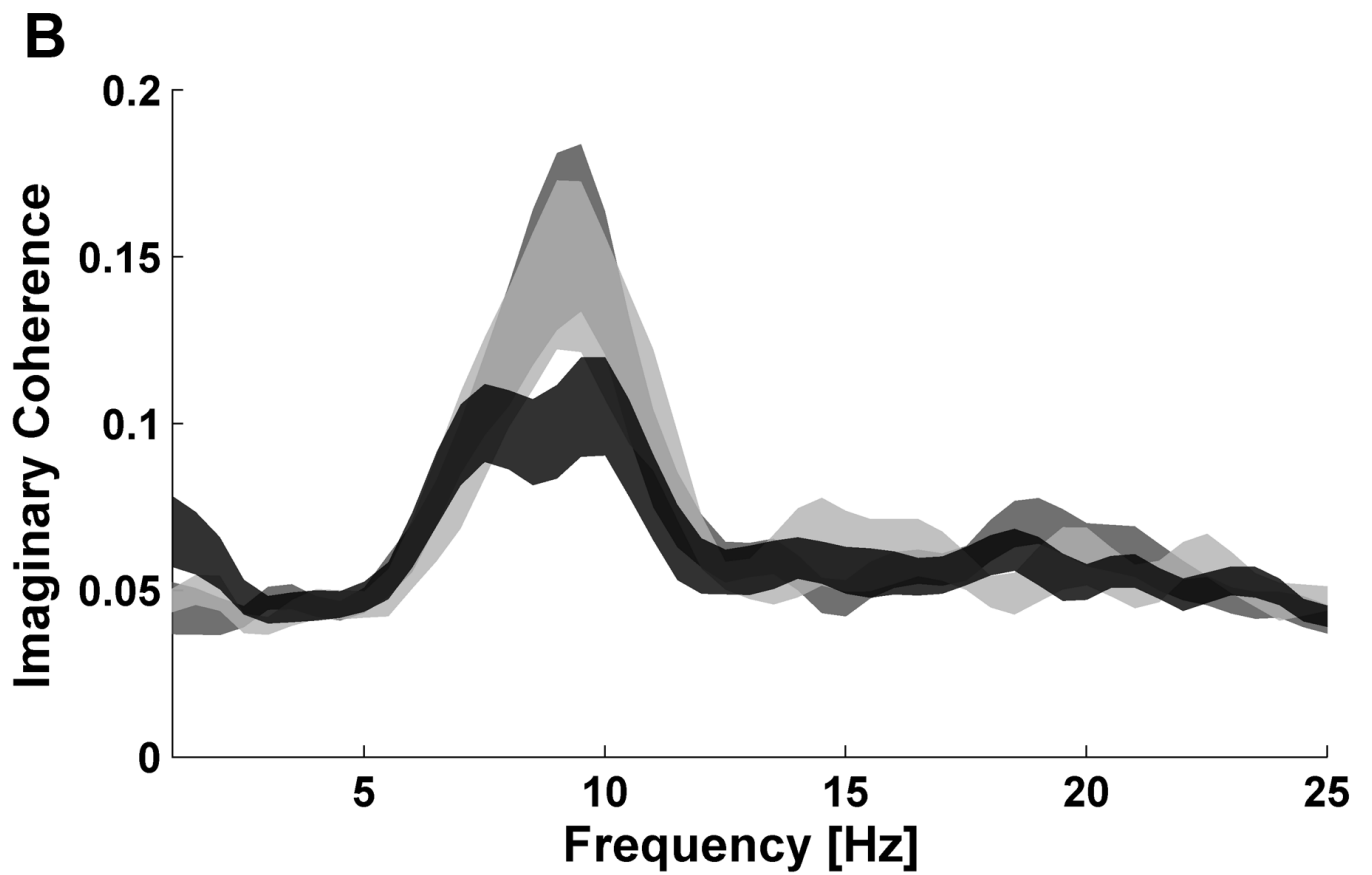
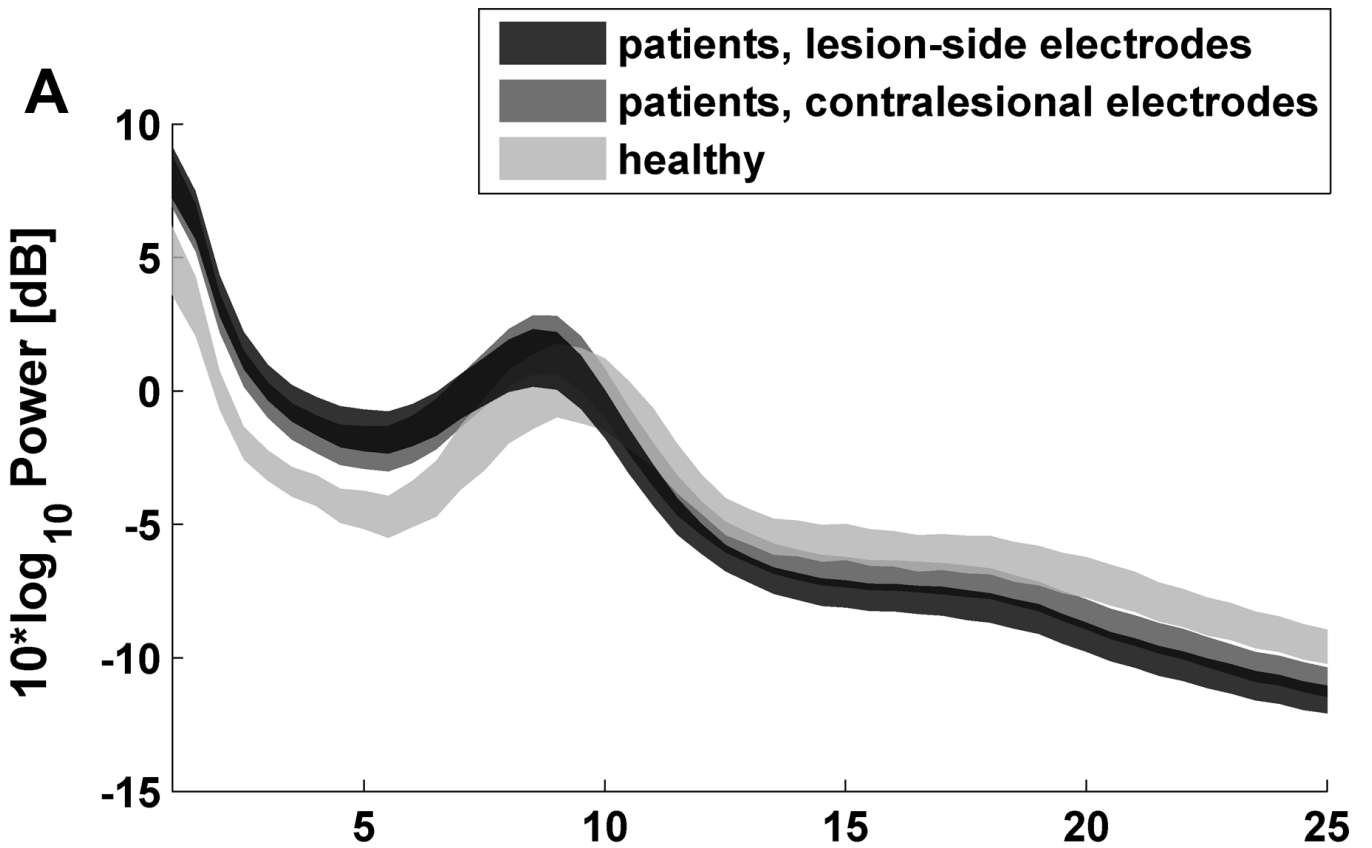


Figure 2

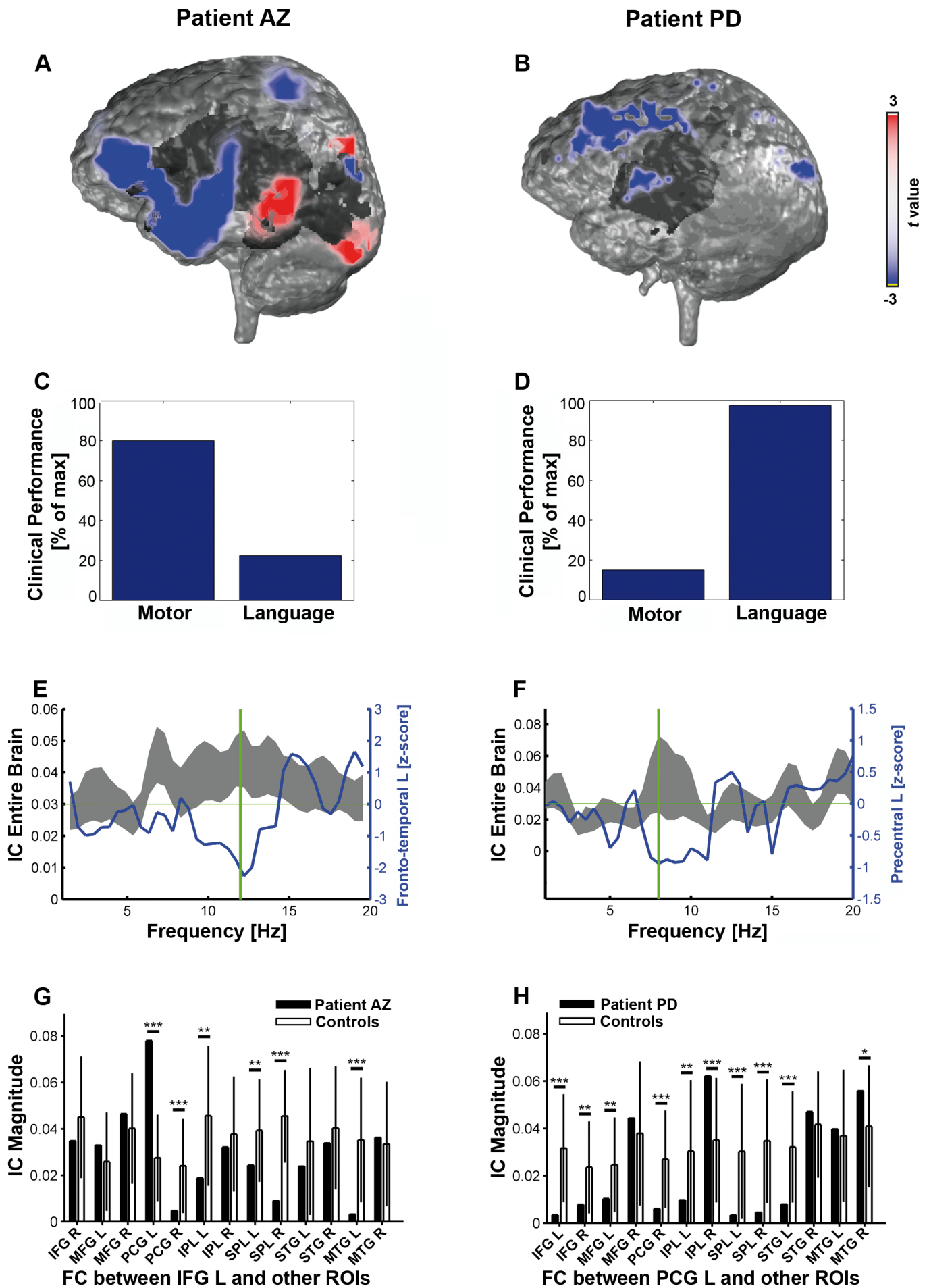
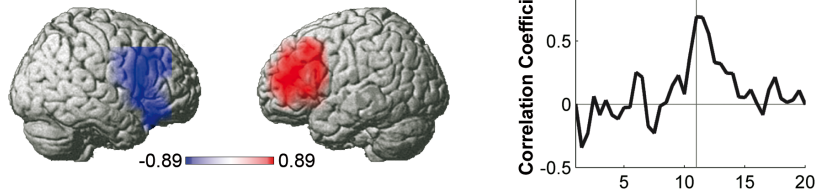
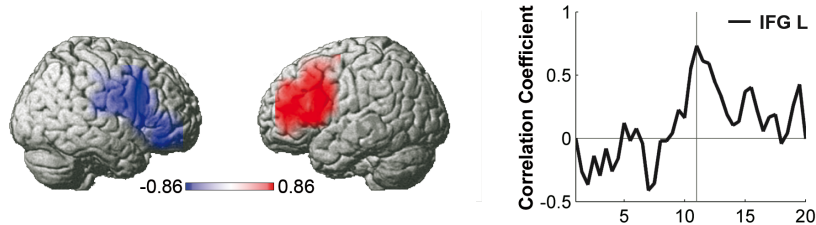


Figure 3

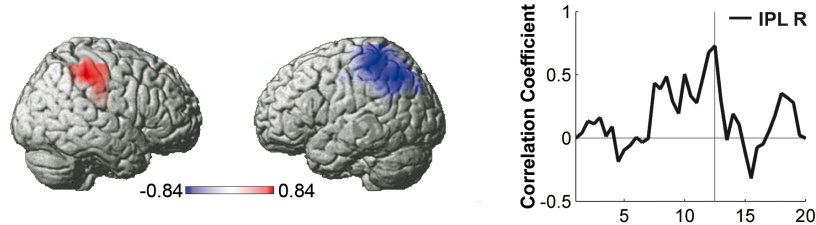
### Verbal Fluency



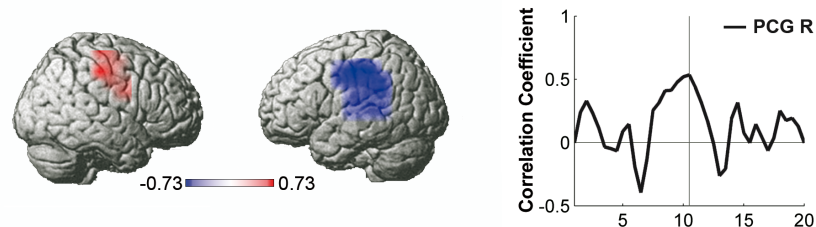
### Verbal Working Memory



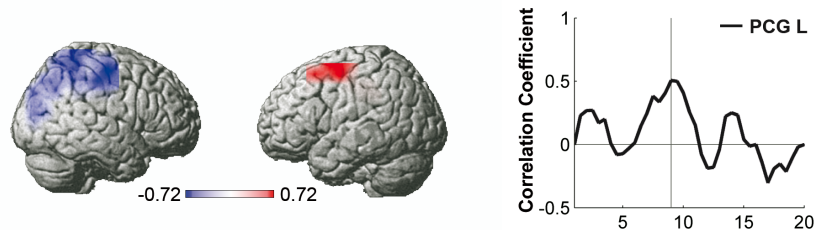
### Spatial Working Memory



### Motor Function (left arm)



### Motor Function (right arm)



### Motor Function (affected arm)

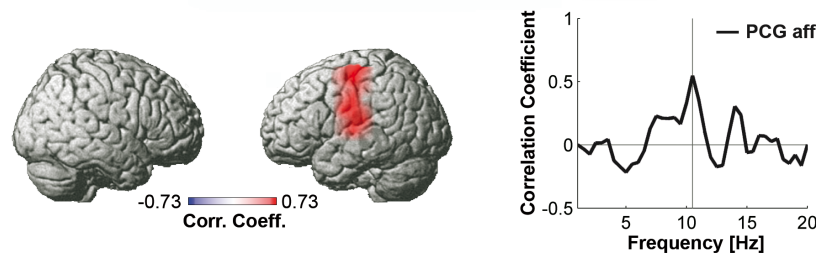


Figure 4

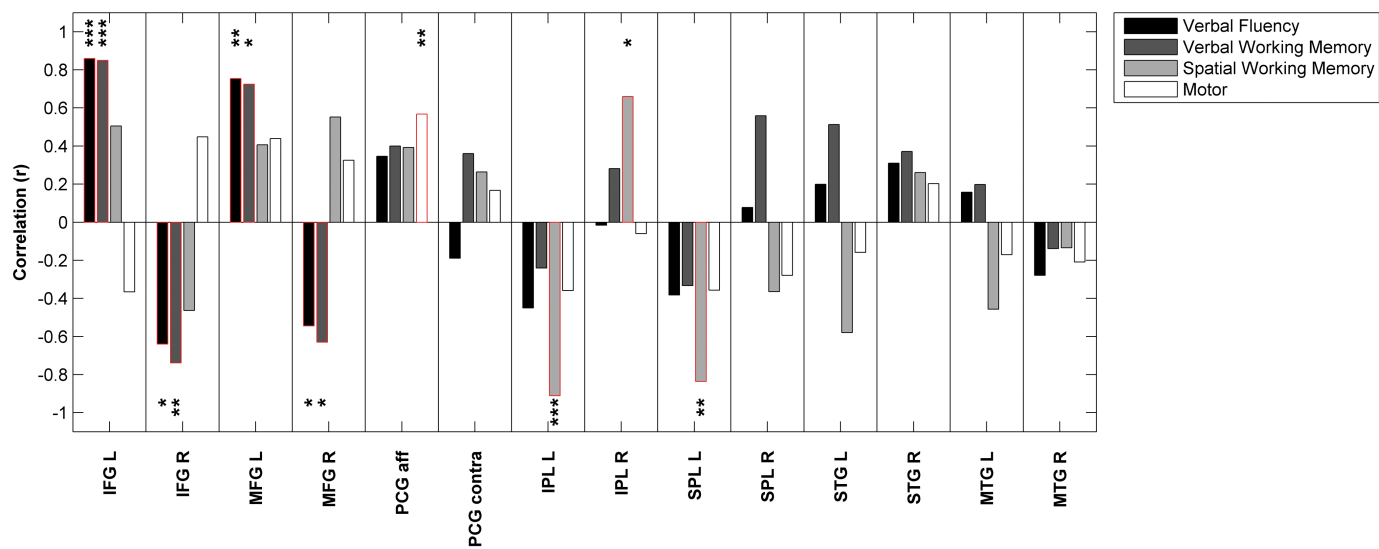
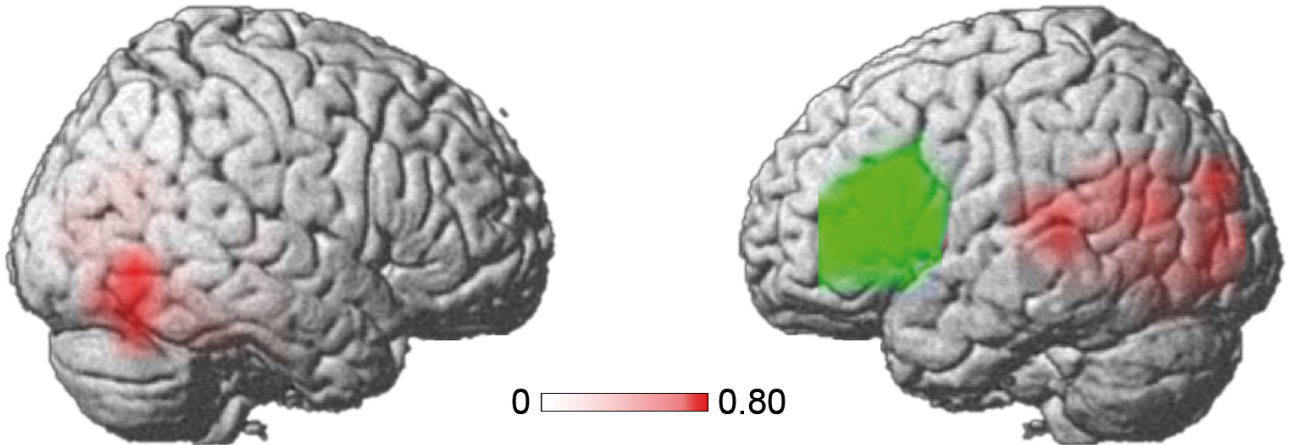
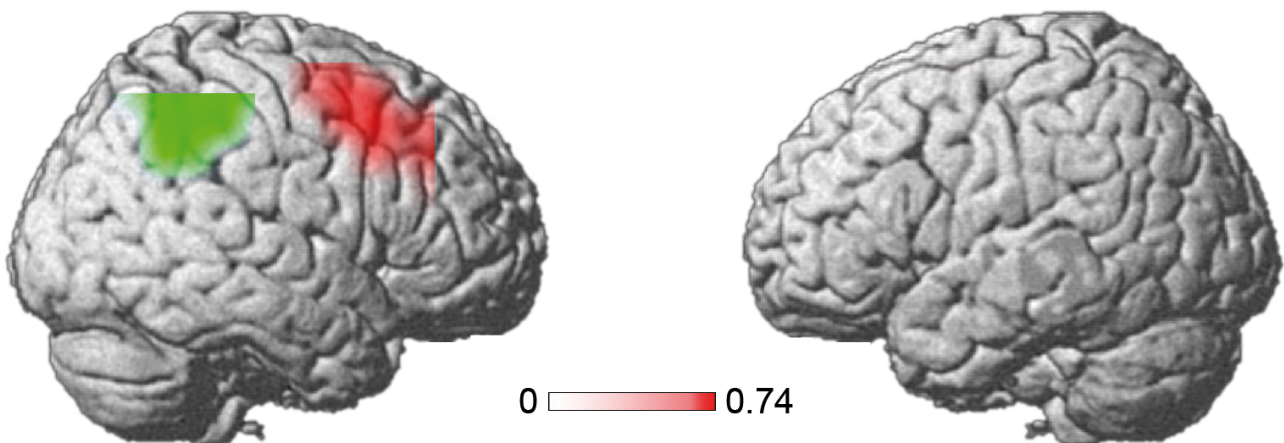


Figure 5

## Verbal Fluency



## Spatial Working Memory



## Motor Function (affected arm)

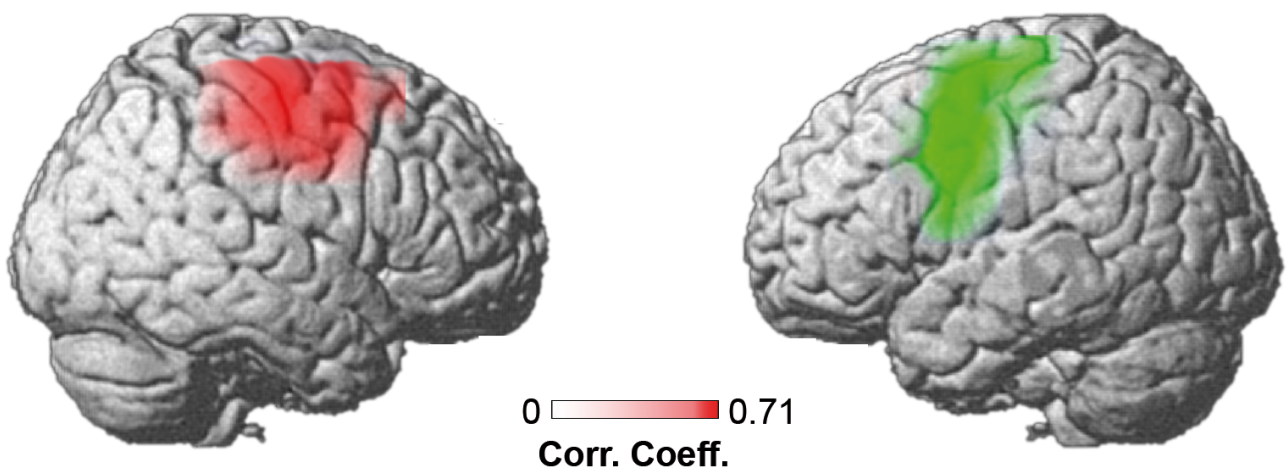


Figure 6

## Supplementary Information to

### The behavioral significance of coherent resting-state oscillations after stroke

*Sviatlana Dubovik<sup>a</sup>, Jean-Michel Pignat<sup>b</sup>, Radek Ptak<sup>a</sup>, Tatiana Aboulafia<sup>b</sup>, Lara Allet<sup>c</sup>, Nicole Gillibert<sup>a</sup>, Cécile Magnin<sup>a</sup>, Fabien Albert<sup>b</sup>, Isabelle Momjian-Mayor<sup>b</sup>, Louis Nahum<sup>a</sup>, Agustina M. Lascano<sup>b</sup>, Christoph M. Michel<sup>b</sup>, Armin Schnider<sup>a</sup>, Adrian G. Guggisberg<sup>a</sup>*

<sup>a</sup> Division of Neurorehabilitation, <sup>b</sup> Division of Neurology, and <sup>c</sup> Unit of Physiotherapy Research and Quality Assurance, University Hospital of Geneva

#### Supplementary Figures

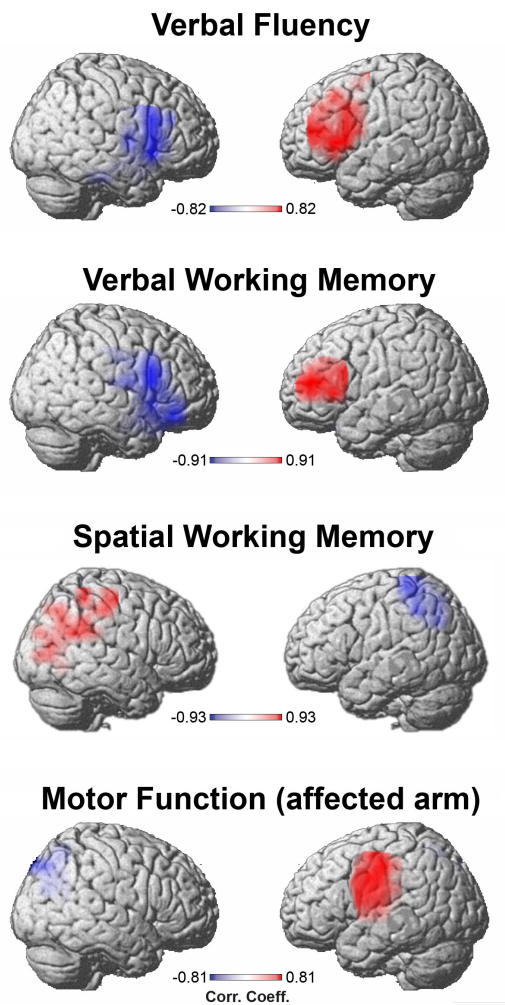
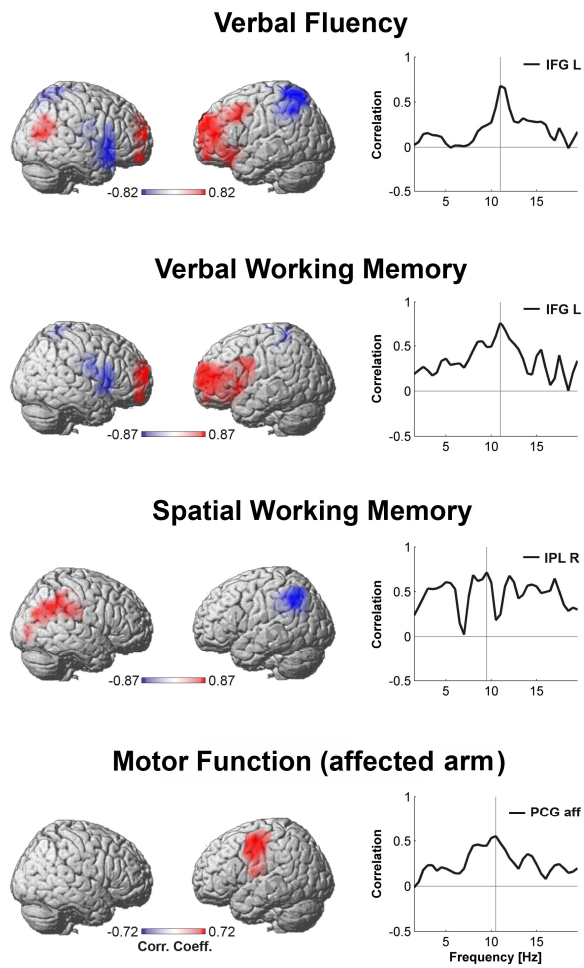


**Figure S1. Partial correlation between FC of each voxel and patient performance, using the age of the patient and the lesion size as co-factors.**

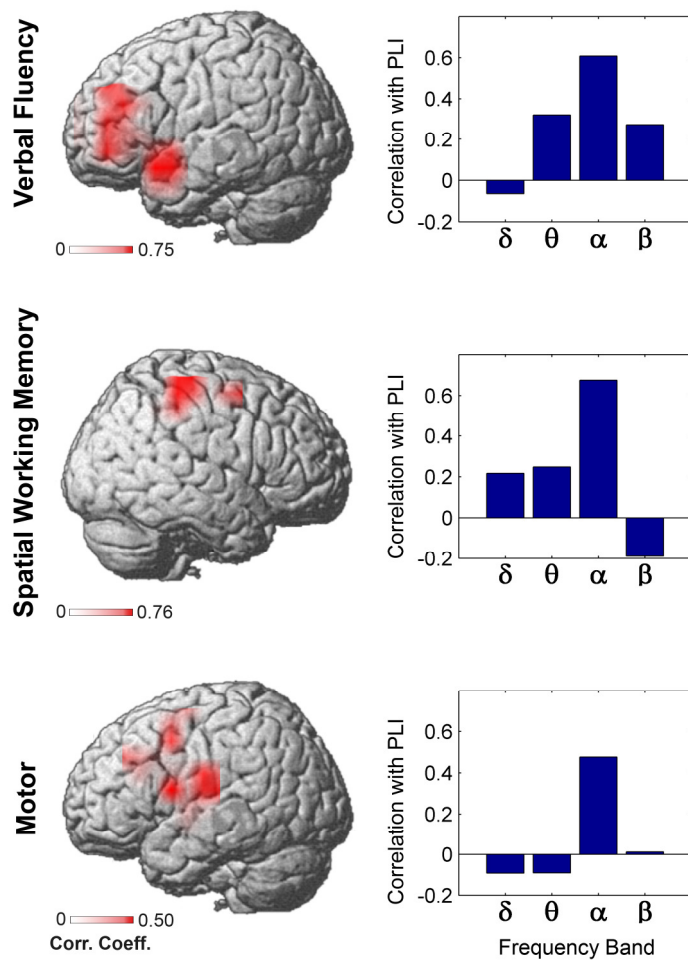
The same regions correlated with neurological function as in the bivariate Pearson correlation analysis shown in Figure 3. This demonstrates that age and stroke severity do not explain the linear relationship between FC and neurological function.

**Figure S2. Magnitude Squared Coherence.**



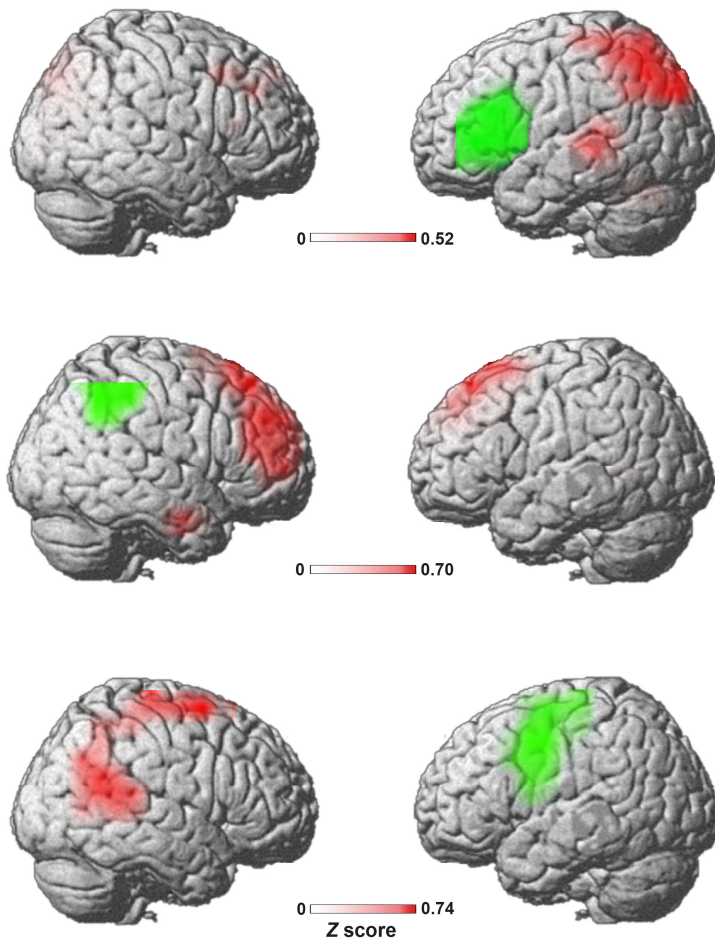
When quantifying FC between brain regions with magnitude squared coherence instead of the imaginary component of coherence (IC) used in the other analyses, we still obtain essentially the same topography of correlations between FC and neurological function. Furthermore, the correlations are again specific to the alpha frequency range. This demonstrates that the usage of IC did not fundamentally alter our results.

**Figure S3. Amplitude-independent quantification of functional connectivity.**



When using an amplitude-independent measure of phase synchrony [the phase lag index (Stam et al., 2007)] to quantify FC instead of the amplitude-sensitive coherence, we still obtain a similar topography of correlations between FC and neurological function. Furthermore, the correlations are again specific to the alpha frequency range. This demonstrates that phase synchrony, not only spectral similarities, in the alpha band are important for cognitive and motor function.

**Figure S4. Alpha synchrony networks in healthy subjects.**



Alpha band interactions which were found to be affected after stroke were examined in 19 healthy subjects. Anatomical ROIs whose FC with other areas was found to be closely related to cognitive and motor function in the patients were selected and used as seed regions (marked in *green*). Areas showing greatest IC with the seed regions are marked in *red* (uncorrected  $p < 0.05$ ). The left IFG interacted most strongly with a left temporal area around the auditory cortex and with the left IPL including the left temporo-parietal junction. The right IPL communicated preferentially with the right middle and superior frontal gyrus. The left motor cortex was most connected with its right counterpart, and with the right parieto-temporal junction. These topographies resemble language, spatial attention, and motor networks observed previously with fMRI (Damoiseaux et al., 2006; Kelly et al., 2010).

## Supplementary Table

**Supplementary Table 1. Demographic and clinical characteristics of the included patients.**

Age	Gender	Lesion Side	Admission NIHSS	Handedness	Suspected Stroke Etiology
67	M	R	13	R	ICA stenosis
51	M	L	15	L	ICA dissection
60	M	L	16	R	cryptogenic
80	F	R	5	R	atrial fibrillation
52	F	R	11	R	primary CNS vasculitis
68	M	R	15	R	cryptogenic
74	F	L	14	R	akinetic left ventricular segment
48	F	L	27	R	cryptogenic
54	F	L	6	R	patent foramen ovale
62	M	R	9	R	ICA occlusion
68	M	R	16	R	atrial fibrillation
37	M	L	8	R	patent foramen ovale and DVT
70	F	L	14	R	atrial fibrillation
53	M	L	20	R	ICA dissection
79	M	R	18	R	ICA occlusion
46	F	R	4	R	cryptogenic
60	M	R	18	R	ICA stenosis
46	M	L	7	R	patent foramen ovale and DVT
73	F	L	3	R	cryptogenic
78	F	R	9	R	atrial fibrillation

Abbreviations: DVT, deep venous thrombosis; ICA, internal carotid artery; NIHSS, National Institute of Health Stroke Scale; M, male; F, female; L, left; R, right.

## Supplementary Methods

### Maps of magnitude squared coherence used in Figure S2

The inverse solutions which need to be applied to reconstruct cortical oscillations from surface EEG/MEG recordings have limited spatial resolution. Hence, the activity reconstructed at each voxel contains not only activity of the voxel itself, but also leaked activity from adjacent areas. Furthermore, this spatial leakage is not homogenous throughout the brain, but varies depending on the location. This introduces artificial similarities among cortical time series leading to overestimations and distortions in the estimated cortical FC. We overcome this problem by calculating the imaginary component of coherence (IC) as measure of FC which ignores similarities occurring with zero time delay (Guggisberg et al., 2008). This takes care of the spatial leakage problem, because the volume conduction leading to spatial leakage spreads with light speed and therefore approaches zero time delay. IC is sensitive only to similarities occurring with non-zero time-delay (Nolte et al., 2004) and is therefore robust to spatial leakage (Guggisberg et al., 2008; Sekihara et al., 2011).

However, when ignoring zero phase delay interactions, we might also miss relevant true neural interactions. In order to test this possibility, we additionally quantified FC with the traditional magnitude squared coherence (which takes into account both zero and non-zero lag interactions) while trying to control for spatial leakage with other means. A previous study has suggested that control for spatial leakage can also be accomplished by subtracting noise FC from the original data FC (Ghuman et al., 2011). Noise FC is obtained by projecting recordings of empty room noise or simulated Gaussian noise through the same spatial filter that was used for the data and calculating FC between these noise source time series. We took a similar but simplified approach, which was based on the observation that, when using long noise datasets, the obtained noise FC approaches the correlation matrix of the spatial filter. The more Gaussian noise we used, the closer the noise correlation was to the correlation between spatial filter weights, up to an almost perfect match when using 5 minutes of simulated Gaussian noise. This means that we could directly subtract the spatial filter correlation matrix from the real component of the data coherence, and obtain the same result as when subtracting noise coherence maps. Simulations confirmed that this provided a good control of the spatial leakage problem.

Another approach to correct for spatial leakage is non-homogeneous smoothing (Schoffelen and Gross, 2011), which was however not used in this study.

### Assessment of alpha synchrony networks in healthy subjects in Figure S4

IC was calculated for all connections of the seed region to the rest of the cortex. IC values were then Fisher-transformed, averaged across the voxels of the seed region, and inverse Fisher-transformed. These FC maps were normalized to the average FC value across all voxels of each subject by calculating z-scores, and spatially normalized to canonical MNI space with SPM8. Average maps were

tested for significance with SnPM permutations and thresholded at uncorrected  $p < 0.05$  to display the full network structure.

## Supporting References

- Damoiseaux, J.S., Rombouts, S.A., Barkhof, F., Scheltens, P., Stam, C.J., Smith, S.M., Beckmann, C.F., 2006. Consistent resting-state networks across healthy subjects. *Proc Natl Acad Sci U S A* 103, 13848-13853.
- Ghuman, A.S., McDaniel, J.R., Martin, A., 2011. A wavelet-based method for measuring the oscillatory dynamics of resting-state functional connectivity in MEG. *Neuroimage* 56, 69-77.
- Guggisberg, A.G., Honma, S.M., Findlay, A.M., Dalal, S.S., Kirsch, H.E., Berger, M.S., Nagarajan, S.S., 2008. Mapping functional connectivity in patients with brain lesions. *Ann. Neurol.* 63, 193-203.
- Kelly, C., Uddin, L.Q., Shehzad, Z., Margulies, D.S., Castellanos, F.X., Milham, M.P., Petrides, M., 2010. Broca's region: linking human brain functional connectivity data and non-human primate tracing anatomy studies. *Eur J Neurosci* 32, 383-398.
- Nolte, G., Bai, O., Wheaton, L., Mari, Z., Vorbach, S., Hallett, M., 2004. Identifying true brain interaction from EEG data using the imaginary part of coherency. *Clin. Neurophysiol.* 115, 2292-2307.
- Schoffelen, J.M., Gross, J., 2011. Improving the interpretability of all-to-all pairwise source connectivity analysis in MEG with nonhomogeneous smoothing. *Hum Brain Mapp* 32, 426-437.
- Sekihara, K., Owen, J.P., Trisno, S., Nagarajan, S.S., 2011. Removal of spurious coherence in MEG source-space coherence analysis. *IEEE Trans Biomed Eng* 58, 3121-3129.
- Stam, C.J., Nolte, G., Daffertshofer, A., 2007. Phase lag index: assessment of functional connectivity from multi channel EEG and MEG with diminished bias from common sources. *Hum Brain Mapp* 28, 1178-1193.